ChemComm

COMMUNICATION

View Article Online
View Journal | View Issue

Cite this: *Chem. Commun.*, 2015, 51, 8273

Received 10th March 2015,
Accepted 7th April 2015

DOI: 10.1039/c5cc01975c

www.rsc.org/chemcomm

A double-enhanced strip biosensor for the rapid and ultrasensitive detection of protein biomarkers†

Chunyan Qin, Wei Wen, Xiuhua Zhang, Haoshuang Gu and Shengfu Wang*

Combining the specific molecular recognition reaction between biotin and streptavidin with a dual-class signal amplification system, containing the unique optical properties of gold nanoparticles and the catalytic reaction of horseradish peroxidase, a double-enhanced strip biosensor was designed for the first time for a visual and rapid detection of protein biomarkers with good accuracy, especially for CEA with a detection limit of 2.9 fg mL^{-1}.

The development of lateral flow biosensors (LFBs) for sensitive point-of-care testing (POCT) of cancer markers for early cancer diagnosis and treatment is a crucial need, primarily in resource-limited settings because they require low volumes of reagents and are easy to use, store and transport.[1] The advantages of proteins as potential disease biomarkers include their enormous diversity and secretion into blood and bodily fluids.[2] Such an enormous diversity of protein forms increases the chances of identifying a marker or a panel of markers for each disease state.[3] However, it also poses the analytical challenge of detecting a specific protein in complex biological matrices.[4] At present, different methods have been applied to test protein biomarkers, such as electrochemical immunosensor, surface plasmon resonance, fluorescence immunoassay,[5] *etc.*

Although all of the above methods offer high sensitivity and accuracy, these analytical techniques require expensive instrumentation and complicated sample pretreatment processes, which limit their real-time and wide onsite applicability. Paper-based analytical devices have recently emerged as ideal platforms.[6] As is well-known, LFBs are simple to manipulate, fast responding, stable long term and inexpensive techniques that are useful for POCT.[7] Therefore, LFBs have been demonstrated to detect carcinoembryonic antigen (CEA), thrombin, microRNA, salmonella, Hg^{2+},[8] *etc.* in *in situ* tests.

To overcome all of the above-mentioned drawbacks and meet the crucial need for the development of a POCT with high sensitivity and specificity for the detection of protein biomarkers, we designed a double-enhanced lateral flow strip biosensor. All previous studies support the use of paper-based strips to achieve the onsite detection of protein biomarkers in a feasible and timely manner, and moreover, a dual-class signal amplification system was designed. The signal amplifying particles were mainly gold nanoparticles (AuNPs) because of their high molar absorption coefficient, accumulating ability and vivid colour, which are caused by localized surface plasmon resonance and excellent chemical stability.[9] Li *et al.* have been engaged in employing gold nanomaterials in electrochemical research and have had brilliant achievements.[10] In addition, the other assisting signal amplification particle was horseradish peroxidase (HRP) due to its high catalytic efficiency, high specificity and manageable enzyme activity.[11] This design produced a large electrical signal amplification effect and provides an unprecedented high sensitivity, a wide linear range and a low detection limit for the POCT of protein biomarkers.

We first selected the CEA as our detection target to verify the feasibility of this method and prepared AuNPs by using the citrate reduction method;[12] then we condensed the AuNPs to different concentrated solutions through centrifugation and chose the 10-fold AuNP solution to prepare the hairpin oligonucleotide (HO)–AuNP–DNA, HRP–AuNP–cDNA (integrally complementary to the corresponding DNA) and cDNA–AuNP conjugates. Moreover, the streptavidin (SA)–cHO (partially complementary to the corresponding loop sequences of HO) conjugates were obtained using previously reported methods.[13] All details are shown in the ESI† (Fig. S1–S4).

The LFB for CEA detection is fabricated as shown in the schematic diagram (Scheme 1A; Fig. S5, ESI†). In a typical assay, sample solutions containing the CEA and HO–AuNP–DNA conjugates are separately applied to the LFB sample pad. The complexes migrate *via* capillary action, as recognition reactions, and the exposed activated biotins are captured by the preimmobilized SA on the TZ to form the first characteristic red band because of the accumulation of AuNPs. The excess complexes continue to migrate to the CZ and are captured *via* hybridization reactions between CEA–HO and cHO. The AuNPs accumulate to produce the second

Hubei Collaborative Innovation Center for Advanced Organic Chemical Materials, Ministry of Education Key Laboratory for the Synthesis and Application of Organic Functional Molecules & College of Chemistry and Chemical Engineering, Hubei University, Wuhan 430062, P. R. China. E-mail: wangsf@hubu.edu.cn

† Electronic supplementary information (ESI) available: Experimental details and additional information. See DOI: 10.1039/c5cc01975c

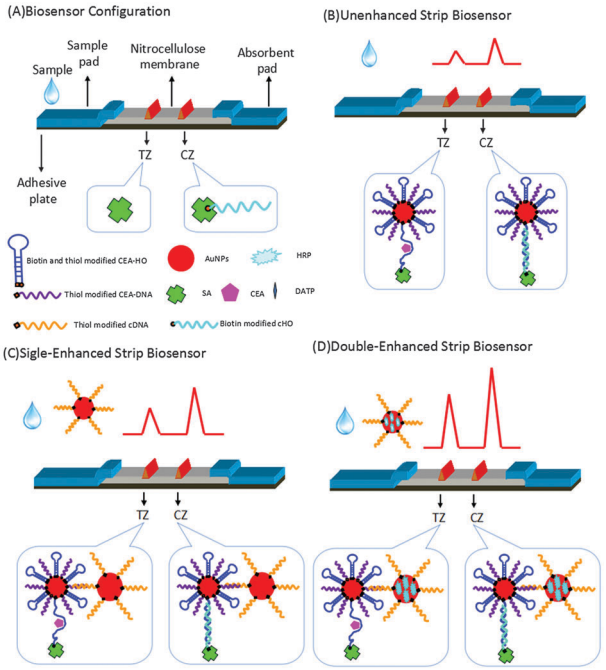

Scheme 1 Schematic illustration of the configuration of the (A) conventional strip biosensor, and the detection of protein biomarkers by the (B) unenhanced, (C) single-enhanced, and (D) double-enhanced strip biosensors.

characteristic red band (Scheme 1B). Three minutes later, the cDNA–AuNP–HRP conjugates are loaded onto the LFB to hybridize with the DNA in the HO–AuNP–DNA conjugates. During this step, the red bands both on the TZ and CZ deepen significantly due to the accumulation of more AuNPs (Scheme 1C). Another three minutes later, the 3-amino-9-ethyl carbazole (AEC) and H_2O_2 complexes are added to the LFB to induce enzyme-catalysed reactions with HRP. Thus, red bands on both the TZ and CZ deepen sharply again (Scheme 1D). In the absence of the CEA, there is only one red band on the control zone, which indicates that the LFB functioned properly.

To determine if the double-enhanced strip biosensor (DSB) has an obvious amplification effect, we compared the DSB with the single-enhanced strip biosensor (SSB) as well as the unenhanced strip biosensor (USB) by studying the 5 ng mL^{-1} CEA. As shown in the photos in Fig. 1A, the colour of the red band on the TZ gradually deepened from the USB to the DSB. In addition, their respective optical responses supported the following conclusion: the DSB has the highest peak area on the TZ (Fig. 1B). These results prove

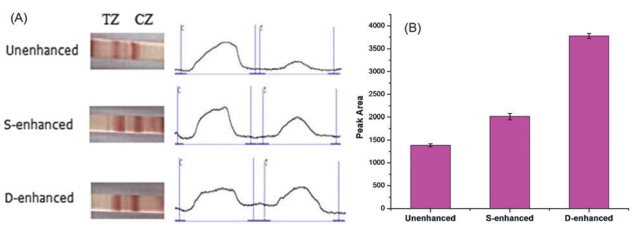

Fig. 1 (A) Typical photo images of the unenhanced, single-enhanced and double-enhanced strip biosensors for the detection of 5 ng mL^{-1} CEA. (B) Their corresponding optical responses.

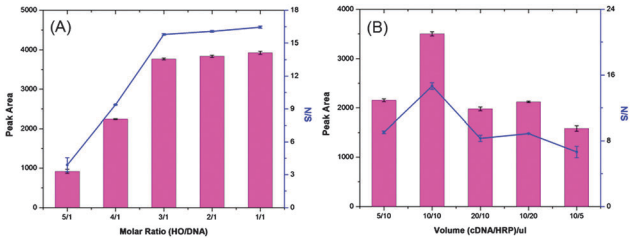

Fig. 2 Effect of different (A) molar ratios of CEA–HO to CEA–DNA and (B) volumes of cDNA and HRP on the responses of the strip biosensor. The histograms represent the peak areas on the test zone, and the blue line represents the S/N ratio (S/N $\geq$ 3) in the presence of the 5 ng mL^{-1} CEA, respectively.

that our strip biosensor is a good amplifier and has a great operation performance due to the signals produced by the AuNP concentration and the dual signal amplification spurred by the AuNP deposition and enzyme catalysis.

The experimental parameters were systematically optimized because they could affect the performance of the LFB. The molar ratio of CEA–HO to CEA–DNA could influence the recognition reaction and complementary strand amplification (Table S1, ESI†). As shown in Fig. 2A, the peak areas on the TZ and the S/N ratios show consistency; both increased with decreasing molar ratios from 5/1 to 3/1, and reached their maxima at 1/1. The volumes of cDNA and HRP can adversely affect the amplification efficiency and result in a decrease of the catalytic efficiency (Table S2, ESI†). As shown in Fig. 2B, the optical intensities and S/N ratios were altered as the volumes of cDNA and HRP changed, and they reached a maximum when they both were 10 μL. To further minimize the nonspecific adsorption and take the cost per assay into account, we chose 1% PBSB, 30 μL DATP, 30 min reaction time between DATP and AuNP labelled conjugates, 20 μL cDNA–AuNP–HRP and 20 μL of AEC–H_2O_2 as the optimized parameters throughout the experiments (Fig. S6, ESI†).

Under the optimized conditions, as shown in Fig. 3A, the red band on the TZ is still visible even at 10 fg mL^{-1} CEA, which can be used as the threshold for the visual detection of the CEA without special instrumentation (visual monitoring: SSB: 50 pg mL^{-1}; USB: 1 ng mL^{-1}). From Fig. 3B, we could determine that the response of the 20 ng mL^{-1} CEA detected using the DSB was still higher than the response of the 200 ng mL^{-1} CEA detected using the other two strip biosensors, the detection limits of the SSB and USB being 9.1 pg mL^{-1} and 0.5 ng mL^{-1}, respectively; however, our DSB has a linear relationship between the peak area and the CEA concentration in the range of 5 fg mL^{-1}–20 ng mL^{-1} with a detection limit of 2.9 fg mL^{-1} (R^2 = 0.98521) (Fig. S7, ESI†), which is 6 orders of magnitude larger than the USB without signal amplification and 3 orders of magnitude larger than the SSB with signal amplification attributed to only AuNP aggregation (Table S3, ESI†).

The mucin 1 protein (MUC1) and thrombin have been used as targets to test and verify the wider applicability of the DSB. As expected, the intensity of the test band increased with the increase in the target concentration to a certain value, and then became saturated at the higher concentration. In Fig. 4, the resulting calibration curves show that the peak areas *versus* the logarithm of

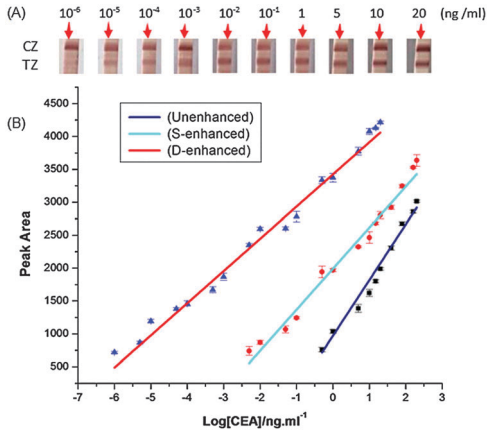

Fig. 3 (A) Photoimages of the detection results of different concentrations of CEA. (B) Calibration curve of the three strip biosensors shows the linear relationship between the peak areas on the test zone *vs.* the logarithm of different CEA concentrations.

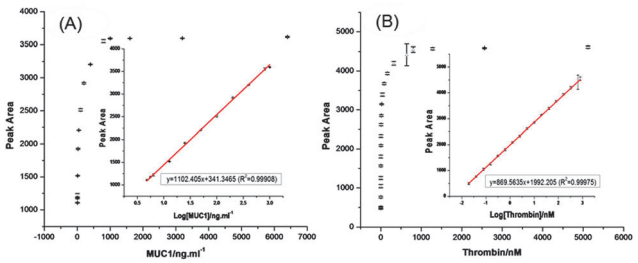

Fig. 4 Plots of the peak areas on the test zone *vs.* different concentrations of protein biomarkers ((A) MUC1; (B) thrombin). Inset displays the linear relationship between the peak areas *vs.* the logarithm of MUC1 (thrombin) concentrations.

the targets are linear over the 4.8 ng mL^{-1}–1.0 μg mL^{-1} range with a detection limit of 1.2 ng mL^{-1} (R^2 = 0.99908; MUC1; Fig. 4A) and the 19 pM–0.8 μM range with a detection limit of 18 pM (R^2 = 0.99975; thrombin; Fig. 4B), which is comparable with other electrochemical detection results (Table S3, ESI†).[14,15]

To implement the detection of the CEA in real human plasma samples, it is essential to assess the analytical selectivity and reproducibility of the DSB against possible interferences in the samples. Typical photoimages (Fig. 5A) and the corresponding peak areas (Fig. S8A, ESI†) both illustrated that this method can detect CEA specifically with negligible interference from other proteins. The strips were stored in sample sacks under desiccated conditions at 4 °C and measured at different times with 5 ng mL^{-1} CEA. Similar colour intensities (Fig. 5B) and responses (Fig. S8B, ESI†) could be obtained from the strip biosensors after the same time. The corresponding RSD values were 7.862%, 0.316% and 0.459%, respectively, indicating excellent analytical stability and reproducibility. Different concentrations of real human plasma samples were detected and further certified using the standard chemiluminescence (CL) method. The results (Table S4, ESI†) revealed insignificant differences, confirming the accuracy of our developed biosensor for detecting CEA.

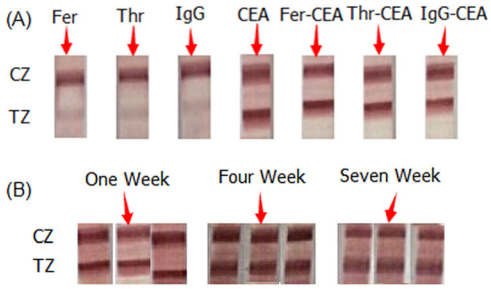

Fig. 5 Typical photoimages of the red band on the test zone (A) detected different proteins (CEA, 5 ng mL^{-1}; other proteins, 100 ng mL^{-1}) (B) detected with 5 ng mL^{-1} CEA at different weeks.

In summary, we have successfully developed double-enhanced strip biosensors for the POCT of protein biomarkers based on AuNP aggregation and HRP-assisted dual-class signal amplification. Given the significant amplification effect, the DSBs are ultrasensitive for the CEA assay with a detection limit of 2.9 fg mL^{-1}, which is 6 orders of magnitude larger than the USB and 3 orders of magnitude larger than the SSB. Moreover, our method offered exquisite selectivity for CEA against other coexisting proteins, and can also be applied in the detection of patient plasma samples, MUC1 and thrombin with good sensitivity and accuracy. These results made it abundantly clear that the principle of the DSB is promising for the rapid identification of other types of proteins and analytes onsite.

This work was supported by the National Natural Science Foundation of China (No. 21175032, 21475032) and the Natural Science Fund for Creative Research Groups of Hubei Province of China (No. 2014CFA015).

Notes and references

1 H. Liu and R. M. Crooks, *J. Am. Chem. Soc.*, 2011, **133**, 17564.
2 D. S. Wishart, T. Jewison and A. C. Guo, *Nucleic Acids Res.*, 2013, **41**, D801.
3 Y. W. Chen, H. L. Xiao and C. Tan, *Practical Journal of Cancer*, 2002, **17**, 116.
4 U. Landegren, J. Vanelid and M. Hammond, *Anal. Chem.*, 2012, **84**, 1824.
5 (*a*) Y. Q. Ge, J. Wu, H. X. Ju and S. Wu, *Talanta*, 2014, **120**, 218; (*b*) J. L. Yuan, G. L. Wang, K. Majima and K. Matsumoto, *Anal. Chem.*, 2001, **73**, l869.
6 R. Pelton, *Trends Anal. Chem.*, 2009, **28**, 925.
7 C. Ma, W. P. Li, Q. K. Kong, H. M. Yang, Z. Q. Bian, X. R. Song, J. H. Yu and M. Yan, *Biosens. Bioelectron.*, 2015, **63**, 7.
8 (*a*) C. C. Ge, L. X. Yu, Z. Y. Fang and L. W. Zeng, *Anal. Chem.*, 2013, **85**, 9343; (*b*) J. H. Chen, S. G. Zhou and J. L. Wen, *Anal. Chem.*, 2014, **86**, 3108.
9 C. M. Li, Y. F. Li, J. Wang and C. Z. Huang, *Talanta*, 2010, **81**, 1339.
10 (*a*) S. J. Xu, Y. Liu, T. H. Wang and J. H. Li, *Anal. Chem.*, 2010, **82**, 9566; (*b*) M. Wang, C. Sun, L. Wang, X. Ji, Y. Bai, T. Li and J. H. Li, *J. Pharm. Biomed. Anal.*, 2003, **33**, 1117; (*c*) Y. Y. Zhao, Z. L. Chen, Y. F. Chen, J. Xu, J. H. Li and X. Y. Jiang, *J. Am. Chem. Soc.*, 2013, **135**, 12940.
11 K. Reddaiah and T. R. Madhusudana, *J. Mol. Liq.*, 2014, **196**, 77.
12 Y. Q. He, S. Zhang, X. Zhang, M. Baloda, A. S. Gurung, H. Xu, X. Zhang and G. D. Liu, *Biosens. Bioelectron.*, 2011, **26**, 2018.
13 Y. Huang, W. Wen, D. Du, X. H. Zhang, S. F. Wang and Y. H. Lin, *Biosens. Bioelectron.*, 2014, **54**, 578.
14 A. K. H. Cheng, H. P. Su, A. Wang and H. Z. Yu, *Anal. Chem.*, 2009, **81**, 6130.
15 Z. Zhu, C. C. Wu, H. P. Liu, C. J. Yang and W. H. Tan, *Angew. Chem., Int. Ed.*, 2010, **49**, 1.